

# Metal-Stabilized Boronate Ester Cages

Erica Giraldi, Rosario Scopelliti, Farzaneh Fadaei-Tirani, and Kay Severin\*

Institut des Sciences et Ingénierie Chimiques, École Polytechnique Fédérale de Lausanne (EPFL), CH-1015 Lausanne, Switzerland

Supporting Information Placeholder

**ABSTRACT:** Molecular cages with arylboronate ester caps at the vertices are described. The cages were obtained by metal-templated polycondensation reactions of a tris(2-formylpyridine oxime) ligand with arylboronic acids. Suited templates are triflate or triflimide salts of Zn<sup>II</sup>, Fe<sup>II</sup>, Co<sup>II</sup>, or Mn<sup>II</sup>. In the products, the metal ions are coordinated internally to the pyridyl and oximate N-atoms adjacent to the boronate ester, resulting in an improved hydrolytic stability of the latter. It is possible to decorate the cages with cyano or aldehyde groups using functionalized arylboronic acids. The aldehyde groups allow for a post-synthetic modification of the cages via imine bond formation.

compounds.<sup>14,16–20,36</sup> Materials based on boronate ester cages are of interest for gas sorption or separation, and cages with BET surface areas of more than 3400 m<sup>2</sup>g<sup>-1</sup> have been reported.<sup>25</sup> A potential drawback for applications is the susceptibility of boronate ester- and boroxine-based cages towards hydrolytic degradation. Attempts have been made to stabilize boronate ester cages by post-synthetic modification (intramolecular alkene metathesis),<sup>24</sup> but the required synthetic efforts are substantial.

Below, we describe the synthesis and the characterization of boronate ester cages, which are stabilized by coordination to internal metal ions (Figure 1c). The cages are less prone to hydrolytic degradation, and the vertices of the cages can be decorated in a flexible fashion with different functional groups.

## Introduction

Boronate ester are formed by condensation of boronic acids with diols.<sup>1</sup> Despite the high thermodynamic stability of the B–O bond, most boronate esters undergo rapid exchange reactions. Therefore, boronate esters can be used as dynamic covalent links in polymer chemistry<sup>2–4</sup> and in structural supramolecular chemistry.<sup>5–9</sup> Molecular cages containing boronate ester links can be obtained by [x+y] polycondensation reactions of appropriately designed polyboronic acids and polyalcohols. Cages with different geometries have been reported, including heterodimeric [1+1] cages,<sup>10</sup> trigonal bipyramidal or trigonal prismatic [2+3] cages,<sup>11–15</sup> cavitand-based [2+4] cages,<sup>16–20</sup> tetrahedral [4+6] cages (an example is depicted in Figure 1a),<sup>21–23</sup> cubic [8+12] cages,<sup>24,25</sup> and a complex interlocked [16+24] cage.<sup>26</sup> Boronate esters have also been combined with dynamic covalent imine bonds to make cages in three-component [2+3+6] polycondensation reactions.<sup>27,28</sup> Furthermore, it is possible to obtain molecular cages with boroxine links by self-condensation of diboronic acids.<sup>29,30</sup>

Boronate esters and boroxines are Lewis acidic compounds, which can form adducts with N-donor ligands.<sup>31,32</sup> The formation of dative B–N bonds can trigger the formation<sup>33</sup> or the interconversion of cages.<sup>30</sup> Dative B–N bonds can also be employed as a structure-directing element for the formation of boronate ester-based cages (an example is depicted in Figure 1b).<sup>34–37</sup>

A characteristic feature of molecules with a cage-like shape is the presence of internal cavity, which allows accommodating guest molecules. Cages featuring boronate ester groups were found to act as hosts for ammonium<sup>10</sup> and caesium ions,<sup>33</sup> for fullerenes,<sup>11</sup> and for (poly)aromatic

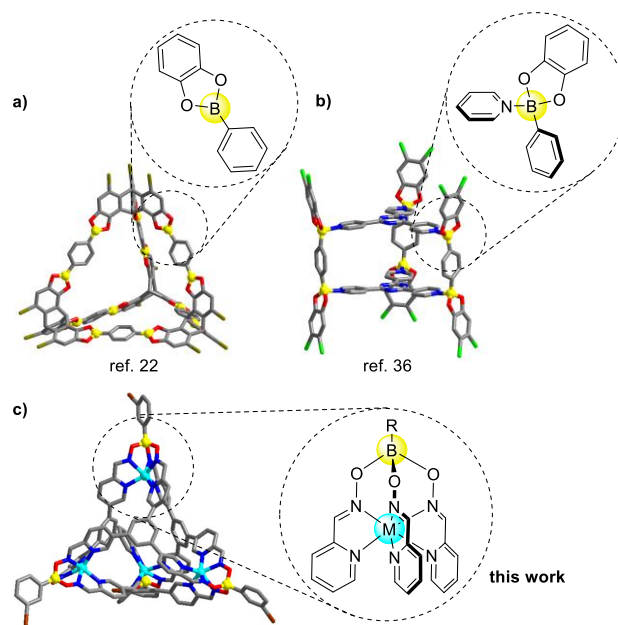


**Figure 1.** Examples of molecular cages containing boronate ester links (a), dative B–N bonds to boronate esters (b), and metal-stabilized boronate esters (c).

## Results and Discussion

Boronate ester-capped metal complexes of type A (Figure 2) were first described by Bosten and Rose in 1968.<sup>38</sup> These complexes classify as 'clathrochelates'<sup>39,40</sup> because the central metal ion is completely surrounded by a macrobicyclic ligand framework.

Boronate-ester capped clathrochelate complexes feature remarkably inert B–O bonds. As a consequence, they don't degrade in aqueous solution, enabling biological applications.<sup>41</sup> On the other hand, they are not suited as constitutionally dynamic links in supramolecular chemistry. However, clathrochelates with additional donor groups in apical position can be used as versatile metalloligands.<sup>42,43</sup>

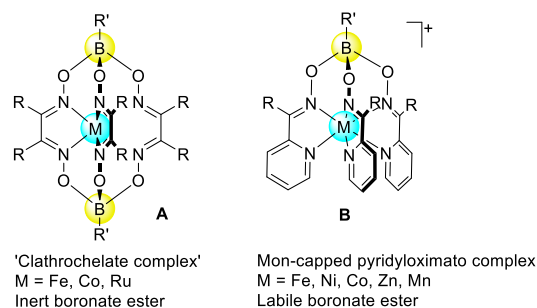
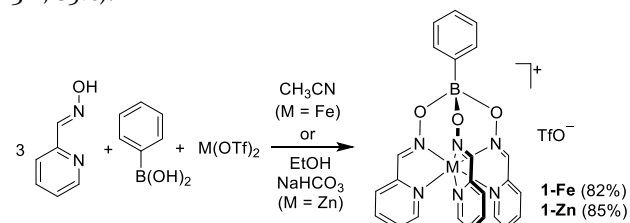


**Figure 2.** General structure of boronate ester-capped clathrochelates (A) and mono-capped pyridyloximato complexes (B).

Complexes of type A are obtained by a metal-templated condensation reaction of a 1,2-dioxime with a boronic acid.<sup>39,40</sup> Using a pyridyloxime instead of a dioxime leads to mono-capped, cationic complexes of type B (Figure 2).<sup>44,45</sup> The reported synthetic procedures indicate that the mono-capped complexes are not prone to hydrolytic degradation (e.g. CH<sub>2</sub>Cl<sub>2</sub> solutions of the Ni<sup>II</sup> complex can be washed with water).<sup>44</sup>

We have recently described first attempts to integrate compounds of type B into more complex molecular architectures. In particular, we have shown that dinuclear complexes with a helicate-like structure can be obtained when ditopic bispyridyloxime ligands were employed instead of simple pyridyloximes.<sup>46</sup> However, there was no information of whether the helicates were formed under kinetic or (partial) thermodynamic control.

Prior to targeting even more elaborate cage structures, we decided to examine the structures and the dynamic behavior of mono-capped pyridyloximato complexes. For this purpose, we synthesized the new complexes **1-Fe** and **1-Zn** by reaction of pyridine-2-aldoxime (3 equiv) with phenylboronic acid (1 equiv) and M(OTf)<sub>2</sub> (1 equiv; M = Fe or Zn) (Scheme 1). For the synthesis of **1-Fe**, acetonitrile was used as solvent (reflux, 90 min, 82% yield). The synthesis of the Zn<sup>II</sup> complex **1-Zn** was accomplished in ethanol in the presence of NaHCO<sub>3</sub> (reflux, 3 h, 85%).



**Scheme 1.** Synthesis of the complexes **1-Fe** and **1-Zn**.

The complexes were characterized by NMR spectroscopy, high-resolution mass spectrometry, and by single crystal X-ray diffraction (Figure 3). Whereas the Zn–N bonds in **1-Zn** are all of similar length (2.13–2.19 Å), one can observe distinct differences between the lengths of the Fe–N<sub>oximato</sub> and the Fe–N<sub>pyridyl</sub> bonds, with the former being 0.1 Å shorter (1.89 vs. 1.99

Å). Another noteworthy difference between **1-Fe** and **1-Zn** is the coordination geometry of the metal ion. For **1-Zn**, one can observe a distorted trigonal prismatic geometry with an average twist angle<sup>47</sup> of  $\phi_{av.} = 14^\circ$ . The coordination geometry of the Fe<sup>II</sup> complex, on the other hand, is better described as distorted octahedral with an average twist angle of  $\phi_{av.} = 40^\circ$ . The different coordination environments of the two complexes also influences the boronate ester capping groups. Due to the increased octahedral character of **1-Fe**, the boron atom is closer to the metal center than in **1-Zn** (2.98 Å for **1-Fe** vs. 3.27 Å for **1-Zn**).

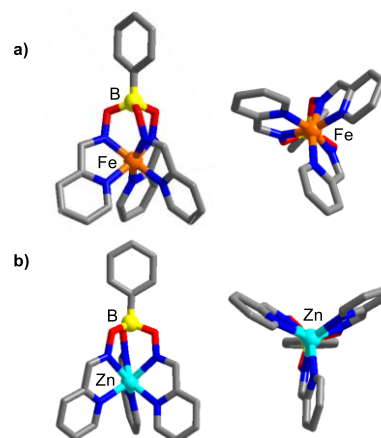
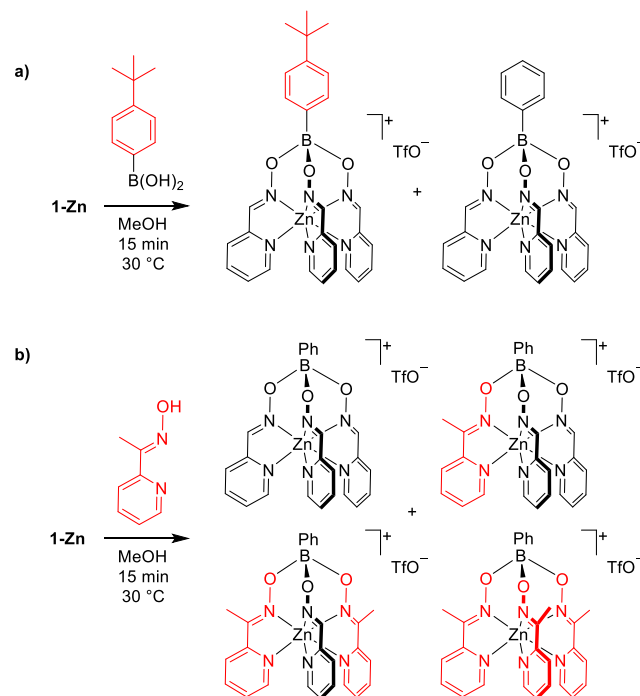


**Figure 3.** Molecular structure of **1-Fe** (a) and **1-Zn** (b) in the crystal, with view from the side and along the M...B axis. Triflate anions and hydrogen atoms are not shown for clarity.

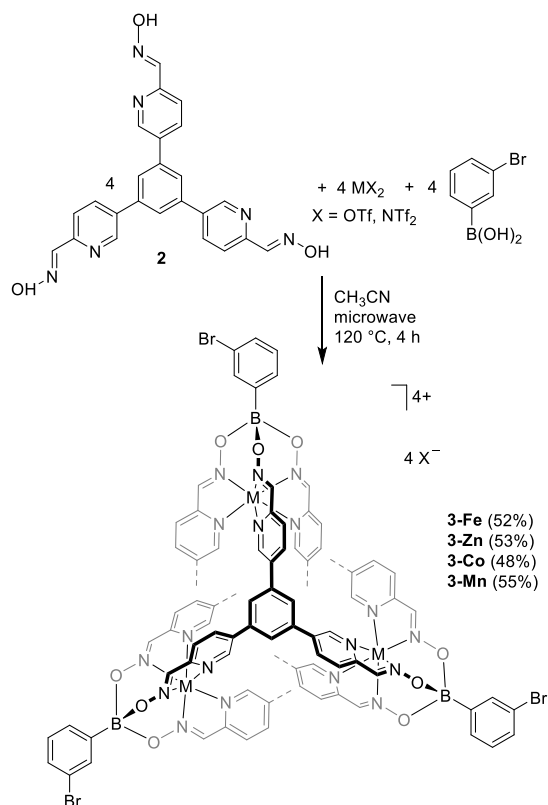


**Scheme 2.** Exchange reactions with 4-*tert*-butylphenylboronic acid (a) and with 2-acetylpyridine oxime (b).

Next, we have investigated the lability of **1-Zn** by performing exchange reactions. Solutions of the complex in methanol or acetonitrile (13 mM) were mixed with 4-*tert*-butylphenylboronic acid (1 equiv) or 2-acetylpyridine oxime (3 equiv) (Scheme 2).

After an equilibration time of 15 min at 30 °C, the resulting mixtures were investigated by mass spectrometry. For the reactions with the boronic acid, we observed approximately equally intense peaks for complexes with phenylboronate ester and with 4-*tert*-butylphenylboronate ester cap (see the Supporting Information, Figures S49 and S50). For the reaction with 2-acetylpyridine oxime, we observed peaks for complexes containing zero, one, two, or three 2-acetylpyridine oximate ligands. These experiments indicate that ligand exchange reactions involving B–O bond rupture are possible for mono-capped pyridyloximate complexes.

Encouraged by these results, we set out to explore if boronate ester cages can be obtained with capped pyridyloximate complexes as links. For this purpose, we have used the tritopic ligand **2** (Scheme 3). This ligand was obtained from the corresponding trialdehyde<sup>48</sup> by condensation with hydroxylamine hydrochloride.



**Scheme 3.** Synthesis of the tetrahedral cages **3-M** ( $M = \text{Fe}, \text{Zn}, \text{Co}, \text{Mn}$ ).

First test reactions with  $\text{MX}_2$  salts ( $X = \text{OTf}$  or  $\text{NTf}_2$ ) and phenylboronic acid showed that tetranuclear condensation products had formed (NMR and/or MS data), but the polycondensation reactions were incomplete. Using the slightly more soluble 3-bromophenylboronic acid and more forcing reaction condition (dry acetonitrile, microwave heating, 120 °C, 4 h) gave improved results, and we were able to obtain the cages **3-M** ( $M = \text{Fe}, \text{Zn}, \text{Co}, \text{Mn}$ ) with isolated yields of approximately 50% after precipitation with diethyl ether (Scheme 3). NMR characterization in solution was possible for the diamagnetic complexes **3-Fe** and **3-Zn**, whereas the paramagnetic<sup>44</sup> complexes **3-Co** and **3-Mn** were analyzed by mass spectrometry. The high-resolution ESI mass spectrum of cage **3-Mn** is characteristic for this kind of assembly and presents three major peaks corresponding to the

cationic cage with a variable number of anions:  $[\mathbf{3-Mn-4OTf}]^{4+}$ ,  $[\mathbf{3-Mn-3OTf}]^{3+}$ , and  $[\mathbf{3-Mn-2OTf}]^{2+}$  (Figure 4).

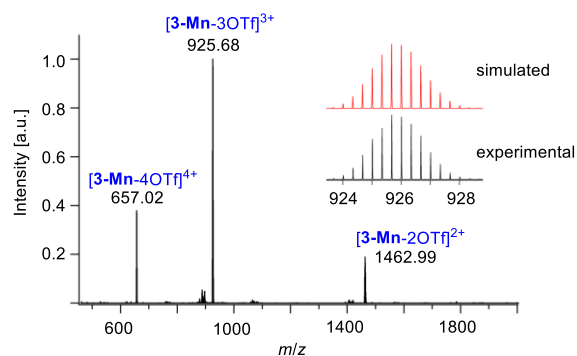


**Figure 4.** HR-MS of cage **3-Mn**, with zoom-in on the isotopic distribution at  $m/z = 926$  (inset).

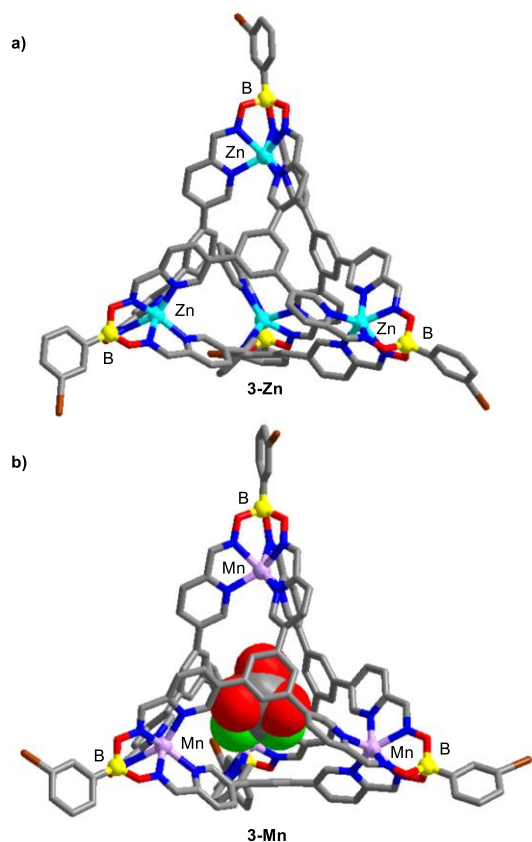
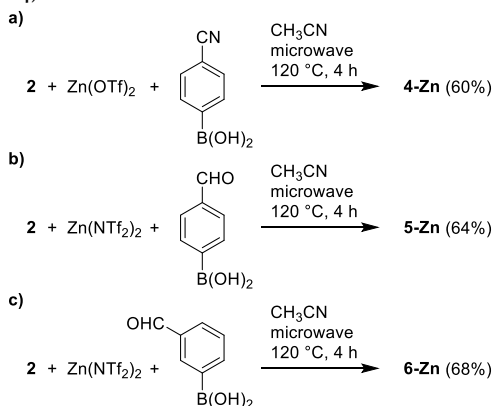


**Figure 5.** Molecular structure of the cationic cages of **3-Zn** (a) and of **3-Mn** with encapsulated  $\text{TfO}^-$  (b) in the crystal. Hydrogen atoms are not shown for clarity.

The molecular structures of **3-Zn** and **3-Mn** were determined by single crystal X-ray diffraction (Figure 5). The diffraction data were of moderate quality, and most of the triflate ions could not be located with accuracy. Only one encapsulated  $\text{TfO}^-$  ion in the cavity of **3-Mn** could be refined (Figure 5b). The coordination environment of the  $\text{Zn}^{\text{II}}$  ions in **3-Zn** is similar to what was observed for the mononuclear complex **1-Zn**: the six N-donor atoms are arranged in a distorted trigonal prismatic fashion ( $\phi_{\text{av.}} = 19^\circ$ ) with an average Zn–N bond length of 2.16 Å. Slightly shorter metal–nitrogen bond distances of  $\text{Mn–N}_{\text{av.}} = 2.11$  Å are found for the  $\text{Mn}^{\text{II}}$  complex **3-Mn**, but the coordination geometry is very similar, with an average twist angle of  $\phi_{\text{av.}} = 19^\circ$ .

The distortion from an ideal trigonal prismatic geometry implies that the four metal centers in **3-Zn** and **3-Mn** are chiral and display the same chirality in the crystal ( $4 \times \Delta$  or  $4 \times \Lambda$ ).

An interesting feature of boronate ester-capped metal cages is the possibility to introduce additional functional groups by using a functionalized boronic acid during the synthesis. <sup>40-43</sup> Tetrahedral cages can also be decorated with pendent functional groups, as evidenced by synthesis of cages with cyano (**4-Zn**) and aldehyde group (**5-Zn** and **6-Zn**, Scheme 4).<sup>49</sup>



**Scheme 4.** Synthesis of zinc cages with pendent cyano (a) and aldehyde groups in para (b) and meta position (c).

The complexes **4-Zn**, **5-Zn**, and **6-Zn** were characterized by NMR spectroscopy and high-resolution mass spectrometry. In addition, we were able to determine the solid state structures of **4-Zn** and **6-Zn** by single crystal X-ray diffraction (Figure 6). The overall geometry of these cages is similar to what was found for **3-Zn**. The cyano groups in **4-Zn** are 2.8 nm apart from each other. It is worth noting that clathrochelate complexes with pendent cyano groups have been used in the past for the synthesis of coordination polymers with unusual network topologies.<sup>50</sup> Cage **4-Zn** could potentially be used as a nanoscale link for creating 4-connected networks. The aldehyde-functionalized cages **5-Zn** and **6-Zn**, on the hand, could serve as building blocks in reactions with amines.<sup>51</sup> However, amine-aldehyde condensations liberate water, and the presence of boronate ester groups in **5-Zn** and **6-Zn** presents a potential obstacle. We thus examined the hydrolytic stability of the cages using **6-Zn** as representative example. Increasing amounts of D<sub>2</sub>O were added to a solution of **6-Zn** in CD<sub>3</sub>CN (2.5 mM). Up to 10 vol% D<sub>2</sub>O were well tolerated. With 15 vol% D<sub>2</sub>O, small amounts of decomposition products could be detected by NMR spectroscopy (SI, Figure S47). Cage **6-Zn** also displays an increased kinetic inertness when compared to the mononuclear complex **1-Zn**: the addition of 4-*tert*-butylphenylboronic acid (4 equiv) to a solution of **6-Zn** in CH<sub>3</sub>CN (5 mM) did lead to only minor exchange of the boronate ester cap, as evidenced by an MS analysis after tempering the mixture for an hour at 50 ° C.

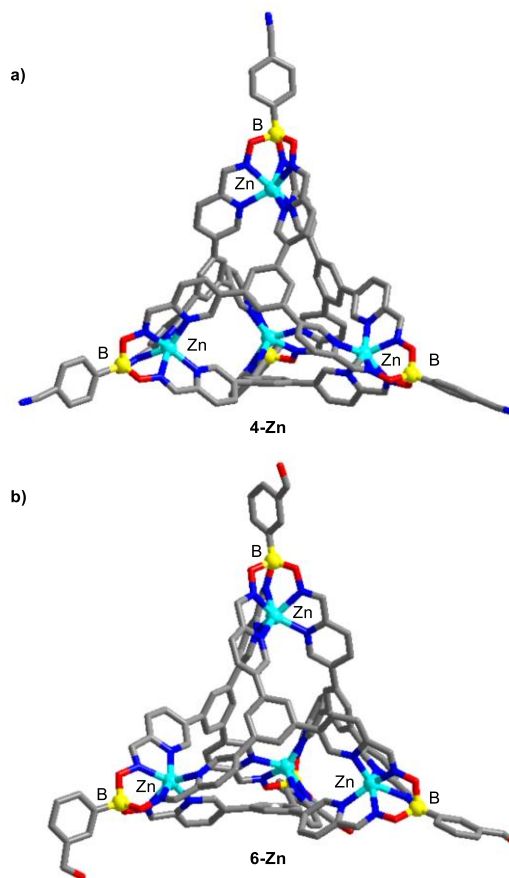
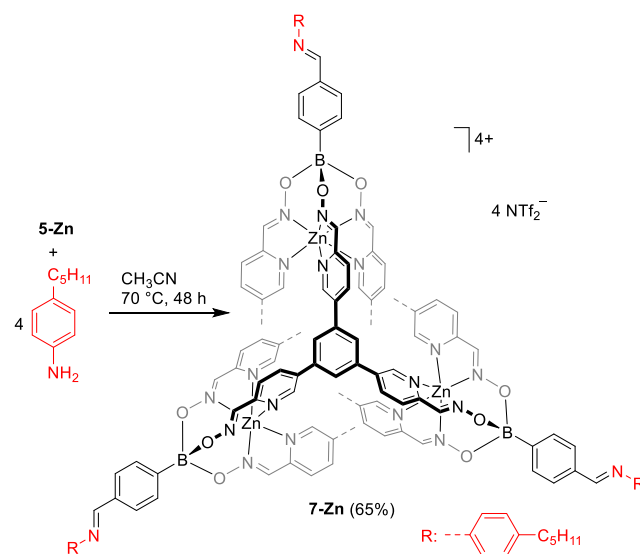


**Figure 6.** Molecular structure of the cationic cages of **5-Zn** (a) and of **6-Zn** (b) in the crystal. Hydrogen atoms are not shown for clarity.



**Scheme 5.** Post-synthetic modification of **5-Zn**.

To demonstrate the feasibility of post-synthetic functionalization<sup>52</sup> via imine bond formation, we have examined the reaction of **5-Zn** with 4-pentylaniline. Imine formation was achieved by heating a solution of the two compounds in acetonitrile for 48 h. The resulting imine-decorated cage **7-Zn** was obtained after precipitation with diethyl ether with an isolated yield of 65% (Scheme 5).

## Conclusion

We have shown that arylboronate ester-capped pyridyloximate complexes are constitutionally dynamic compounds, which are able to undergo exchange reactions with boronic acids and pyridyl oxime ligands. This feature makes them well suited for the construction of complex supramolecular structures. By using a tris(2-formylpyridine oxime) ligand, we have been able to obtain tetrahedral cages with boronate ester caps in metal-templated polycondensation reactions. Due to the presence of internally coordinated  $M^II$  ions, the cages display an increased hydrolytic stability when compared to purely organic cages with boronate ester or boroxine links. On the other hand, the presence of metal ions introduces charges and counter ions. The latter can occupy the cage cavity and potential external voids. Consequently, it is unlikely that assemblies based on boronate ester-capped pyridyloximate complexes will lead to materials with permanent porosity, as it was observed for some charge-neutral boronate ester cages.<sup>25</sup> It is also worthwhile to compare the new cages with a tetrahedral imine cage (**8-Zn**), which was obtained by a  $Zn^{2+}$ -templated condensation of a phenyl-centered tris(2-formylpyridine) ligand with tris(2-aminoethyl)amine (tren).<sup>53</sup> This imine cage is structurally similar to the  $Zn^{2+}$  cages described here, even though its cavity is a bit smaller (see SI, Figure S54). One difference is the reduced charge of our cages (4+) compared to the imine cage (8+), which could influence solubility and host-guest chemistry. An advantage of boronate ester caps compared to tren-based caps is the possibility to introduce functional groups at the cage vertices by using appropriate boronic acid. Functionalized cages could be used as nanoscale building blocks for more complex molecular assemblies or polymeric materials.<sup>54,55</sup>

## ASSOCIATED CONTENT

### Supporting Information

The Supporting Information is available free of charge on the ACS Publications website at <http://pubs.acs.org>.

Experimental procedures and analytical data of the ligands and cages (<sup>1</sup>H, <sup>13</sup>C, DOSY NMR, HRMS) in Figure S1–S54.

### Accession Codes

Crystallographic data for the structures reported in this paper have been deposited at the Cambridge Crystallographic Data Center (CCDC) as supplementary publications CCDC 2061750 (**3-Zn**), 2061751 (**3-Mn**), 2061752 (**4-Zn**), 2061753 (**6-Zn**), 2080461 (**1-Fe**), 2080462 (**1-Zn**).

## AUTHOR INFORMATION

### Corresponding Author

\* To whom correspondence should be addressed.

E-mail: [kay.severin@epfl.ch](mailto:kay.severin@epfl.ch).

### ORCID

Erica Giraldi: 0000-0001-7655-4585

Rosario Scopelliti: 0000-0001-8161-8715

Farzaneh Fadaei-Tirani: 0000-0002-7515-7593

Kay Severin: 0000-0003-2224-7234

### Notes

The authors declare no competing financial interests.

## ACKNOWLEDGMENT

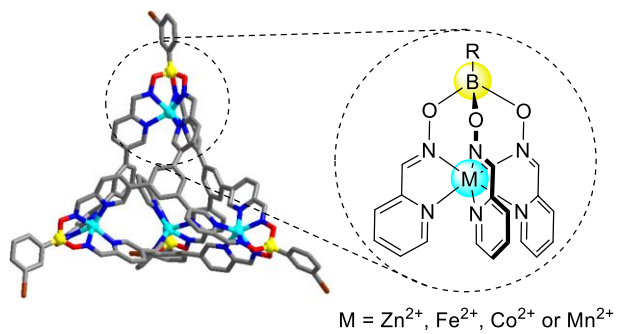
The work was supported by the Swiss National Science Foundation and by the Ecole Polytechnique Fédérale de Lausanne (EPFL).

## REFERENCES

- Hall, D. G. *Boronic Acids*, 2<sup>nd</sup> Ed., Wiley-VCH, Weinheim, 2011.
- Nakahata, M.; Sakai, S. Cross-Linking Building Blocks Using a "Boronate Bridge" to Build Functional Hybrid Materials. *ChemNanoMat* 2019, 5, 141–151.
- Brooks, W. L. A.; Sumerlin, B. S. Synthesis and Applications of Boronic Acid-Containing Polymers: From Materials to Medicine. *Chem. Rev.* 2016, 116, 1375–1397.
- Vancoillie, G.; Hoogenboom, R. Synthesis and polymerization of boronic acid containing monomers. *Polymer Chem.* 2016, 7, 5484–5495.
- Severin, K. Boronic acids as building blocks for molecular nanostructures and polymeric materials. *Dalton Trans.* 2009, 5254–5264.
- Nishiyabu, R.; Kubo, Y.; James, T. D.; Fossey, J. S. Boronic acid building blocks: tools for self-assembly. *Chem. Commun.* 2011, 47, 1124–1150.
- Kubo, Y.; Nishiyabu, R.; James, T. D. Hierarchical supramolecules and organization using boronic acid building blocks. *Chem. Commun.* 2015, 51, 2005–2020.
- de Jesus Hiller, N.; Amaral e Silva, N. A. d.; Tavares, T. A.; Faria, R. X.; Eberlin, M. N.; de Luna Martins, D. Arylboronic Acids and their Myriad of Applications Beyond Organic Synthesis. *Eur. J. Org. Chem.* 2020, 4841–4877.
- Beuerle, F.; Gole, B. Covalent Organic Frameworks and Cage Compounds: Design and Applications of Polymeric and Discrete Organic Scaffolds. *Angew. Chem. Int. Ed.* 2018, 57, 4850–4878.
- Kataoka, K.; James, T. D.; Kubo, Y. Ion Pair-Driven Heterodimeric Capsule Based on Boronate Esterification: Construction and the Dynamic Behavior. *J. Am. Chem. Soc.* 2007, 129, 15126–15127.
- Leonardt, V.; Fimmel, S.; Krause, A.-M.; Beuerle, F. A covalent organic cage compound acting as a supramolecular shadow mask for the regioselective functionalization of C<sub>60</sub>. *Chem. Sci.* 2020, 11, 8409.
- Schäfer, N.; Bühler, M.; Heyer, L.; Röhr, M. I. S.; Beuerle, F. Endohedral Hydrogen Bonding Templates the Formation of a Highly Strained Covalent Organic Cage Compound. *Chem. Eur. J.* 2021, 27, 6077–6085.
- Shan, Z.; Wu, X.; Xu, B.; Hong, Y.-I.; Wu, M.; Wang, Y.; Nishiyama, Y.; Zhu, J.; Horike, S.; Kitagawa, S.; Zhang, G. Dynamic Transformation between Covalent Organic Frameworks and Discrete Organic Cages. *J. Am. Chem. Soc.* 2020, 142, 21279–21284.
- Takata, H.; Ono, K.; Iwasawa, N. Controlled release of the guest molecule via borate formation of a fluorinated boronic ester cage. *Chem. Commun.* 2020, 56, 5613–5616.
- Takahagi, H.; Fujibe, S.; Iwasawa, N. Guest-Induced Dynamic Self-Assembly of Two Diastereomeric Cage-Like Boronic Esters. *Chem. Eur. J.* 2009, 15, 13327–13330.
- Nishimura, N.; Kobayashi, K. Self-Assembly of a Cavitand-Based Capsule by Dynamic Boronic Ester Formation. *Angew. Chem. Int. Ed.* 2008, 47, 6255–6258.
- Nishimura, N.; Yoza, K.; Kobayashi, K. Guest-Encapsulation Properties of a Self-Assembled Capsule by Dynamic Boronic Ester Bonds. *J. Am. Chem. Soc.* 2010, 132, 777–790.
- Nishimura, N.; Kobayashi, K. Self-Assembled Boronic Ester Cavitand Capsule as a Photosensitizer and a Guard Nanocontainer against Photochemical Reactions of 2,6-Diacetoxanthracene. *J. Org. Chem.* 2010, 75, 6079–6085.
- Mitsui, M.; Higashi, K.; Takahashi, R.; Hirumi, Y.; Kobayashi, K. Enhanced photostability of an anthracene-based dye due to supramolecular encapsulation: a new type of photostable fluorophore for single-molecule study. *Photochem. Photobiol. Sci.* 2014, 13, 1130–1136.
- Tamaki, K.; Ishigami, A.; Tanaka, Y.; Yamanaka, M.; Kobayashi, K. Self-Assembled Boronic Ester Cavitand Capsules with Various Bis(catechol) Linkers: Cavity-Expanded and Chiral Capsules. *Chem. Eur. J.* 2015, 21, 13714–13722.
- Klotzbach, S.; Beuerle, F. Shape-Controlled Synthesis and Self-Sorting of Covalent Organic Cage Compounds. *Angew. Chem. Int. Ed.* 2015, 54, 10356–10360.
- Elbert, S. M.; Regenauer, N. I.; Schindler, D.; Zhang, W.-Z.; Rominger, F.; Schröder, R. R.; Mastalerz, M. Shape-Persistent Tetrahedral [4+6] Boronic Ester Cages with Different Degree of Fluoride Substitution. *Chem. Eur. J.* 2018, 24, 11438–11443.
- Klotzbach, S.; Scherpf, T.; Beuerle, F. Dynamic covalent assembly of tribenzotriquinacenes into molecular cubes. *Chem. Commun.* 2014, 50, 12454–12457.
- Hählsler, M.; Mastalerz, M. A Gaint [8+12] Boronic Ester Cage with 48 Terminal Alkene Units in the Periphery for Postsynthetic Alkene Metathesis. *Chem. Eur. J.* 2021, 27, 233–237.
- (a) Zhang, G.; Presly, O.; White, F.; Oppel, I. M.; Mastalerz, M. A Permanent Mesoporous Organic Cage with an Exceptionally High Surface Area. *Angew. Chem. Int. Ed.* 2014, 53, 1516–1520; (b) Ivanova, S.; Köster, E.; Holstein, J. J.; Keller, N.; Clever, G. H.; Bein, T.; Beuerle, F. Isoreticular Crystallization of Highly Porous Cubic Covalent Organic Cage Compounds, *Angew. Chem. Int. Ed.* 2021, DOI: 10.1002/anie.202102982.
- Zhang, G.; Presly, O.; White, F.; Oppel, I. M.; Mastalerz, M. A Shape-Persistent Quadruply Interlocked Giant Cage Catenane with two Distinct Pores in the Solid State. *Angew. Chem. Int. Ed.* 2014, 53, 5226–5230.
- Christinat, N.; Scopelliti, R.; Severin, K. Multicomponent Assembly of Boronic Acid Based Macrocycles and Cages. *Angew. Chem. Int. Ed.* 2008, 47, 1848–1852.
- Içli, B.; Christinat, N.; Tönnemann, J.; Schüttler, C.; Scopelliti, R.; Severin, K. Synthesis of Molecular Nanostructures by Multicomponent Condensation Reactions in a Ball Mill. *J. Am. Chem. Soc.* 2009, 131, 3154–3155.
- Ono, K.; Johmoto, K.; Yasuda, N.; Uekusa, H.; Fujii, S.; Kiguchi, M.; Iwasawa, N. Self-Assembly of Nanometer-Sized Boroxine Cages from Diboronic Acids. *J. Am. Chem. Soc.* 2015, 137, 7015–7018.
- Ono, K.; Shimo, S.; Takahashi, K.; Yasuda, N.; Uekusa, H.; Iwasawa, N. Dynamic Interconversion between Boroxine Cages Based on Pyridine Ligation. *Angew. Chem. Int. Ed.* 2018, 57, 3113–3117.
- Höpfel, H. The tetrahedral character of the boron atom newly defined—a useful tool to evaluate the N→B bond. *J. Organomet. Chem.* 1999, 581, 129–149.
- Korich, A. L.; Iovine, P. M. Boroxine chemistry and applications: A perspective. *Dalton Trans.* 2010, 39, 1423–1431.
- Kataoka, K.; Okuyama, S.; Minami, T.; James, T. D.; Kubo, Y. Amine-triggered molecular capsule using dynamic boronate esterification. *Chem. Commun.* 2009, 1682–1864.
- Dhara, A.; Beuerle, F. Reversible Assembly of a Supramolecular Cage Linked by Boron-Nitrogen Dative Bonds. *Chem. Eur. J.* 2015, 21, 17391–17396.
- Hutin, M.; Bernardinelli, G.; Nitschke, J. R. An Iminoboronate Construction Set for Subcomponent Self-Assembly. *Chem. Eur. J.* 2008, 14, 4585–4593.
- Içli, B.; Sheepwash, E.; Riis-Johannessen, T.; Schenk, K.; Filinchuk, Y.; Scopelliti, R.; Severin, K. Dative boron–nitrogen bonds in structural supramolecular chemistry: multicomponent assembly of prismatic cages. *Chem. Sci.* 2011, 2, 1719–1721.
- For crystalline networks of cages, see: Stephens, A. J.; Scopelliti, R.; Fadaei Tirani, F.; Solari, E.; Severin, K. Crystalline Polymers Based on Dative Boron–Nitrogen Bonds and the Quest for Porosity. *ACS Materials Lett.* 2019, 1, 3–7.
- Boston, D. R.; Rose, N. J. An Encapsulation Reaction. Synthesis of the Clathro Chelate 1,8-Bis(fluoroboro)-2,7,9,14,15,20-hexaoxa-3,6,10,13,16,19-hexaaza-4,5,11,12,17,18-hexamethylbicyclo[6.6.6]eicosa-3,5,10,12,16,18-hexaeneocobalt(III) Ion. *J. Am. Chem. Soc.* 1968, 90, 6859–6860.
- Voloshin, Y. Z.; Belaya, I. G.; Kramer, R. K. Cage Metal Complexes; Clathrochelates Revisited; Springer International Publishing: New York, 2017.
- Voloshin, Y. Z.; Kostromina, N. A.; Kramer, R. K. Clathrochelates: Synthesis, Structure and Properties; Elsevier Science: Amsterdam, The Netherlands, 2002.
- Voloshin, Y. Z.; Novikov, V. V.; Nelyubina, Y. V. Recent advances in biological applications of cage metal complexes. *RSC Adv.* 2015, 5, 72621–72637.

- (42) Jansze, S. M.; Severin, K. Clathrochelate Metalloligands in Supramolecular Chemistry and Materials Science. *Acc. Chem. Res.* **2018**, *51*, 2139–2147.
- (43) Wise, M. D.; Severin, K. Functionalised Clathrochelate Complexes – New Building Blocks for Supramolecular Structures. *Chimia* **2015**, *69*, 191–196.
- (44) Pavlos, A. A.; Savkina, S. A.; Belov, A. S.; Nelyubina, Y. V.; Efimov, N. N.; Voloshin, Y. Z.; Novikov, V. V. Trigonal Prismatic Tris-pyridineoximate Transition Metal Complexes: A Cobalt(II) Compound with High Magnetic Anisotropy. *Inorg. Chem.* **2017**, *56*, 6943–6951.
- (45) Structurally related 'pseudoclathrochelate' complexes based on pyrazolyloximate ligands are also known. For example, see: Varzatskii, O. A.; Penkova, L. V.; Kats, S. V.; Dolganov, A. V.; Vologzhanina, A. V.; Pavlov, A. A.; Novikov, V. V.; Bogomyakov, A. S.; Nemykin, V. N.; Voloshin, Y. Z. Chloride Ion-Aided Self-Assembly of Pseudoclathrochelate Metal Prs-pyrazoloximates. *Inorg. Chem.* **2014**, *53*, 3062–3071.
- (46) Giralardi, E.; Depallens, A.B.; Ortiz, D.; Fadaei-Tirani, F.; Scopelliti, R.; Severin, K. Boronate Ester-Capped Helicates. *Chem. Eur. J.* **2020**, *26*, 7578–7582.
- (47) Zhang, J.; Li, J.; Yang, L.; Yuan, C.; Zhang, Y.-Q.; Song, Y. Magnetic Anisotropy from Trigonal Prismatic to Trigonal Antiprismatic Co(II) Complexes: Experimental Observation and Theoretical Prediction. *Inorg. Chem.* **2018**, *57*, 3903–3912.
- (48) Castilla, A. M.; Ousaka, N.; Bilbeisi, R. A.; Valeri, E.; Ronson, T. K.; Nitschke, J. R. High-Fidelity Stereochemical Memory in a Fe<sup>II</sup><sub>4</sub>L<sub>4</sub> Tetrahedral Capsule. *J. Am. Chem. Soc.* **2013**, *135*, 17999–18006.
- (49) For the synthesis of **5-Zn** and **6-Zn**, Zn(NTf<sub>2</sub>)<sub>2</sub> was employed instead of Zn(OTf)<sub>2</sub>. The utilization of triflimide salts leads to cages with an improved solubility.
- (50) Marmier, M.; Cecot, G.; Vologzhanina, A. V.; Bila, J. L.; Zivkovic, I.; Ronnow, H. M.; Nafradi, B.; Solari, E.; Pattison, P.; Scopelliti, R.; Severin, K. Dinuclear clathrochelate complexes with pendent cyano groups as metalloligands. *Dalton Trans.* **2016**, *45*, 15507–15516.
- (51) Belowich, M. E.; Stoddart, J. F. Dynamic imine chemistry. *Chem. Soc. Rev.* **2012**, *41*, 2003–2024.
- (52) Zeng, H.; Stewart-Yates, L.; Casey, L. M.; Bampos, N.; Roberts, D. A. Covalent Post-Assembly Modification: A Synthetic Multipurpose Tool in Supramolecular Chemistry. *ChemPlusChem* **2020**, *85*, 1249–1269.
- (53) Castilla, A. M.; Ronson, T. K.; Nitschke, J. R. Sequence-Dependent Guest Release Triggered by Orthogonal Chemical Signals. *J. Am. Chem. Soc.* **2016**, *138*, 2342–2351.
- (54) For polymers containing cages as network junctions, see ref. 55 and cited work.
- (55) Li, R.-J.; Pezzato, C.; Bertone, C.; Severin, K. Light-induced assembly and disassembly of polymers with Pd<sub>n</sub>L<sub>2n</sub>-type network junctions. *Chem. Sci.* **2021**, *12*, 4981–4984.

## Table of Contents



**Synopsis:** Molecular cages with arylboronate ester caps at the vertices are formed in metal-templated polycondensation reactions of a tris(2-formylpyridine oxime) ligand with arylboronic acids. Suited templates are triflate or triflimide salts of Zn<sup>II</sup>, Fe<sup>II</sup>, Co<sup>II</sup>, or Mn<sup>II</sup>. The cages can be decorated with cyano or aldehyde groups using functionalized arylboronic acids.